CHAPTER 4

IMPACT OF NANOCELLULOSE-STABILIZED PICKERING NANOEMULSION ON β-CAROTENE BIOACCESSIBILITY IN FOOD SYSTEMS

4.1. Introduction

According to estimates, the world's banana production increased from 69 MT in 2000–2002 to 116 MT in 2017–2019 (OECD/FAO, 2020). One of the main agricultural residues that are released into the environment after harvesting of bananas is the stalk on which the fingers are attached. Researchers have expressed interest in employing rachis fibrillar material in a variety of items in recent years. Nanocellulose, derived from biomass, is gaining attention as a sustainable alternative in various industries due to its excellent physical properties and renewable nature (Lu et al., 2021). They are utilized in Pickering emulsions as eco-friendly stabilizers, particularly due to their anisotropic fiber structure, enabling effective oil/water interface stabilization at low concentrations (Khan et al., 2018). Moreover, nanocelluloses serve as promising carriers for bioactive agents, benefiting from their altered physicochemical properties at the nanoscale, which enhances bioavailability (Casanova et al., 2021).

In recent years, there has been a significant focus on designing emulsions for the regulated release of bioactive chemicals into the bloodstream and gastrointestinal tract (Shah, Zhang, Li, & Li, 2016). Pickering emulsions (PEs), which are stabilised at the oil-water interface by solid particles, are being studied for use in food systems. Solid particles that are frequently utilised for stabilising Pickering emulsions contain safe inorganic particles including silica, calcium carbonate, and hydroxyapatite, as well as food-grade organic components like protein, lipid, and carbohydrate particles (Yang et al., 2017). They provide benefits over conventional surfactant-stabilized emulsions by reducing toxicity issues. These PEs, formed through irreversible binding of particles at the interface, exhibit enhanced stability over time, attributed to the steric barrier of particles hindering coalescence (Shah et al., 2016). Moreover, PEs can be tailored to encapsulate various bioactive compounds, with studies exploring nanoparticle encapsulation at the liquid-

liquid interface or dispersion into the oil phase (Wei et al., 2022; Winuprasith et al., 2018). Several sources of nanocellulose are utilised in the stabilisation of PEs, including banana peels (Costa et al., 2018), pistachio shells (Kasiri & Fathi, 2018), ginkgo shells (Ni et al., 2020), lemon seeds (Zhang et al., 2020), bamboo shoots (He et al., 2020), etc.

Lipid-soluble pigments called carotenoids are present in a wide variety of fruits and vegetables, such as kale, tomatoes, and carrots. They are valued for their taste, color, and health advantages (Park et al., 2018). Among them, β-carotene stands out as a crucial nutrient due to its bioactivities (Weber & Grune, 2012). Extensive research has focused on incorporating β-carotene into foods, employing various delivery systems such as nanoparticles, gels, and emulsions to enhance its stability and bioavailability (Mao, Wang, Liu, & Gao, 2018). Despite its health benefits, the restricted bioavailability and poor oxidative stability of β-carotene pose challenges for its utilization in functional foods. Therefore, encapsulating β-carotene in lipid-based delivery systems has become common practice to address these limitations (McClements, 2018; Liu et al., 2018). Food emulsions have emerged as promising delivery systems for β-carotene, as they allow for its incorporation into oil droplets, thereby enhancing its absorption when co-ingested with lipids (McClements, 2010). This approach improves the bioavailability of β-carotene, facilitating its absorption by epithelial cells and potentially contributing to improved human health outcomes (Wei et al., 2020; Liu et al., 2018).

Mayonnaise is a widely consumed condiment comprising of a stable emulsion of oil and water, traditionally stabilised by egg components such as the white and yolk (Akhtar & Masoodi, 2022). However, the high oil content and egg components in traditional mayonnaise pose limitations for individuals with cardiovascular diseases and egg allergies. To address this, Pickering nanoemulsion (PNE), incorporating solid particles during preparation for its utilization in mayonnaise, offer a solution by stabilizing the emulsion and reducing interfacial tension between oil and water phases. Researchers have stabilised mayonnaise-like emulsions using polysaccharides and plant protein particles (Hosseini et al., 2020), impacting their stability and physicochemical properties such as viscosity, texture, and rheology (Liu et al., 2018). Use of banana rachis nanocellulose (BRNC) as a stabilizer in food system has not been reported. There is feasibility of incorporating PNE of sunflower oil infused with β-carotene and stabilised with BRNC, into emulsion-based gels, such as mayonnaise, to improve β-carotene stability and solubility. Therefore,

incorporating and exploring BRNC will be a promising strategy for improving the stability and nutritional profile of mayonnaise, while catering to diverse dietary needs and preferences.

This study explored the possible utilization of waste material generated after banana harvest in stabilising Pickering nanoemulsion as an eco-friendly stabilizer in food systems. The mechanisms underlying the stabilization effects of BRNC on β-carotene-enriched PNE were explored. Stabilization of PNE was done through a two-step homogenization method aimed at optimizing particle size, PDI, and stability to enhance bioavailability. The main purpose was to use BRNC as a potential stabilizer in PNE and then developing a novel mayonnaise incorporating β-carotene-infused PNE. The resulting β-carotene infused PNE mayonnaise underwent thorough characterization, encompassing assessments of color, texture, rheology, oxidative stability, and qualitative and quantitative analysis.

4.2. Materials and methods

4.2.1. Materials

Cellulose was extracted from freshly harvested and fully mature banana rachis (*Musa acuminata*, 'Dwarf Cavendish') sourced from local farmers in Tezpur, following the isolation method used in a previous study (Basumatary & Mahanta, 2023). Tween-80 (Sigma-Aldrich, purity >99%) along with sunflower oil and standard β-carotene (purity ≥ 93%) were utilized in the study. Analytical chemicals were sourced from TCI, SRL, and Merck.

4.2.2. Preparation and characterization of Pickering nanoemulsion

4.2.2.1. Optimization design

Response Surface Methodology (RSM) with a Box-Behnken three-level design (BBD) model in Design Expert 13.0 (Stat-Ease, Inc., MN) was used to optimize nanoemulsion conditions. **Table 4.1** displays the coded levels and independent variables, varying oil content (5-10%), Tween 80 concentration (5-10%), and nanocellulose concentration (1-3%) as per **Table 4.2**. Responses studied included particle size, polydispersity index (PDI), and emulsion stability, measured using a DLS instrument (Nano Plus, Particulate systems,

GA 30093–2901. U.S.A.). Analysis of variance (ANOVA) with a p-value <0.05 assessed the model's significance.

Table 4.1. Independent variables and their corresponding coded levels

Independent variables	Symbol	Coded levels		
		-1	**0**	**+1**
Oil content (%)	X_1	5	7.5	10
Tween 80 concentration (%)	X_2	5	7.5	10
Nanocellulose concentration (%)	X_3	1	2	3

Table 4.2. Experimental runs for the development of Pickering nanoemulsion

Runs	Experimental Factors		
	A: Oil content	B: Tween 80 concentration	C: Nanocellulose concentration
	(%)	(%)	(%)
1	5	10	2
2	10	7.5	3
3	10	7.5	1
4	5	7.5	3
5	7.5	7.5	2
6	7.5	7.5	2
7	5	7.5	1
8	7.5	7.5	2
9	7.5	7.5	2
10	7.5	10	1
11	7.5	5	1
12	5	5	2
13	7.5	10	3
14	10	10	2
15	10	5	2
16	7.5	7.5	2
17	7.5	5	3

4.2.2.2. Pickering nanoemulsion formulation

Pickering nanoemulsion (PNE) was synthesised by using the optimal conditions for oil content, Tween 80 concentration, and nanocellulose concentration in the organic phase, with minor modifications (Begum et al., 2024). First, using a homogenizer (IKA, Model - T25, Digital Ultra Turrax) set at 11,000 rpm for 5 min, the organic phase comprising different amounts of BRNC, sunflower oil, and Tween 80 was homogenised. This made it easier for the phases to blend and mix at room temperature, producing coarse oil-in-water emulsions. A two-stage high-pressure homogeniser (GEA, Lab homogeniser Panda Plus 2000, Italy) was then used to homogenise the well-mixed coarse emulsion for five passes at 200–500 MPa in order to reduce the particle size to the nanoscale. The selection of five passes was determined through trial and error to achieve a fine oil-in-water nanoemulsion. After that, the generated PNEs were put in glass vials and kept at room temperature for further investigation.

4.2.2.3. Evaluation of Pickering nanoemulsion stability

Evaluation of the stability of the emulsions over 35 days of storage was made by visual observation. Freshly prepared emulsion stabilized with nanocellulose was prepared and kept at ambient temperature for a period of 35 days. Emulsions were stored in centrifuge tubes. The tubes were visually observed at an interval of 7 days for any phase separation and sedimentation.

4.2.2.4. Particle size analysis of Pickering nanoemulsion

PNE particle size was determined by means of Dynamic Light Scattering (DLS). during storage for 0, 5, 10, 15, 20, 25, 30, and 35 days. DLS measurements were done using a NanoPlus instrument from Particulate Systems (GA 30093–2901, U.S.A.) with the following parameters: a general calculation model for irregular particles, a temperature of 25°C, a viscosity of 0.8872 cP, a particle absorption coefficient of 0.01; a particle refractive index of 1.59; and a water refractive index of 1.33.

4.2.2.5. Morphology of Pickering nanoemulsion

Image of the emulsions was obtained with an optical microscope (Nikon Eclipse ME 600 digital microscope, Nikon Instruments Inc., Japan) equipped with Image Pro Plus 5.0

software. Imaging was performed within 30 min after homogenization. The pipette tip was used to pipette a droplet of undiluted emulsion onto a glass slide and spread gently. Cover glass was avoided and was directly used for image acquisition. Emulsions were examined at magnifications of 100X.

4.2.3. Encapsulation of β-carotene in Pickering nanoemulsion

A β-carotene suspension (0.1%, w/w) was dispersed in sunflower oil using a method previously outlined (Wei et al., 2022), with modifications, at 140°C for 30 seconds to initiate the formation of the oil phase. Subsequently, continuous stirring using a magnetic stirrer (Abdos, India) was employed for 1 h at room temperature in a light-free environment to ensure complete dissolution. The oil content was encapsulated with β-carotene at varying concentrations while maintaining other parameters constant. Preparation of Pickering nanoemulsion (PNE) involved blending β-carotene-enriched sunflower oil (5-10%), Tween 80 (5-10%), and nanocellulose concentration (1-3%) under optimized conditions depending on stability, polydispersity index (PDI), and particle size, using the two-step homogenization procedure described in **section 4.2.2.2.** The PNEs, labelled as S1, S2, S3, S4, S5, and S6 based on β-carotene concentrations of 0.02, 0.04, 0.06, 0.08, 0.1, and 0.12 g/10 mL, respectively Freshly prepared β-carotene encapsulated PNEs were promptly refrigerated and used to prepare mayonnaise the following day. The sample container was thoroughly covered with aluminium foil throughout the experimental period to prevent exposure to light.

4.2.4. Chemical stability of β-carotene in Pickering nanoemulsion

The β-carotene nanoemulsion's resistance to degradation during UV light exposure was evaluated in order to determine the chemical stability of the emulsion. The β-carotene content within the PNE was determined using a method outlined in previous studies (Wei & Gao, 2016; Xia et al., 2022). Cuvettes containing nanoemulsion samples were first diluted with deionized water and placed under a controlled UV light chamber (RELITECH, China). Absorbance at 450 nm was measured using a Varian Cary 60 Scan UV-Visible spectrophotometer (Agilent Technologies, Inc, Australia), and a standard curve was used to calculate the amount of β-carotene present in the PNE. The degradation of β-carotene in PNEs is reported as $C/ C_{0.}$ Here, C_0 represents the starting β-carotene content at the preparation stage of nanocellulose particle stabilized β-carotene-loaded

PNE, and C represents the β-carotene content after a specific period of storage (t) under UV light.

4.2.5. Preparation of β-carotene-enriched functional mayonnaise

Preliminary tests were conducted to determine the suitable mayonnaise formulation. Batches of 100 g were prepared as outlined in **Table 4.3**. Using a Hand Mixer (Philips HR3705/10, China), the water phase was blended under vacuum for 15 s after adding sugar, salt, and egg yolk. After that, sunflower oil was added gradually while mixing. PNEs with varying β-carotene concentrations (0.02 – 0.12 g) stabilized with BRNC were gradually added. Vinegar and other ingredients were then blended for an additional minute. The water used for the β-carotene enriched PNE was deducted from the formulation's total water content. After addition of PNEs (S1, S2, S3, S4, S5, and S6), the corresponding mayonnaises were coded as MS1, MS2, MS3, MS4, MS5, and MS6. Prepared mayonnaise samples were stored in glass jars at room temperature (20°C ± 5). Samples were taken on days 0, 7, and 14 for analysis. Mayonnaise without β-carotene served as the control.

4.2.6. Functional mayonnaise characterization

4.2.6.1. Color analysis

A Hunter Colorimeter (Ultrascan Vis, HunterLab, Reston, Virginia, USA) was used to analyse the colour of the functional mayonnaise. The results are shown as b* (yellowness), a* (redness), and L* (lightness). Colour brightness is indicated by L*, and the green-red axis is represented by a* (negative for greenness, positive for redness). The b* value represents the blue-yellow axis (positive for yellowness, negative for blueness) (Roman et al., 2022). The initial color of freshly made mayonnaise was measured, and samples were analysed for color on days 1, 7, and 14 of storage.

4.2.6.2.Morphological analysis

The structure of functional mayonnaise was examined using a Nikon Eclipse ME 600 digital optical microscope (Nikon Instruments Inc., Japan) equipped with Image Pro Plus 5.0 software.

Table 4.3. Different formulation of β-carotene enriched mayonnaise

Sample	**Ingredients (%w/w)**									
	Sunflower oil	PNEs	Water	Egg yolk	Sugar	Salt	Vinegar	Mustard	Pepper	Lime juice
Control	55	-	28.7	5.6	1.3	1	4	1.5	0.3	2.6
MS1	41	15 (S1)	28.7	4.6	1.3	1	4	1.5	0.3	2.6
MS2	40	16 (S2)	28.7	4.6	1.3	1	4	1.5	0.3	2.6
MS3	39	17 (S3)	28.7	4.6	1.3	1	4	1.5	0.3	2.6
MS4	38	18 (S4)	28.7	4.6	1.3	1	4	1.5	0.3	2.6
MS5	37	19 (S5)	28.7	4.6	1.3	1	4	1.5	0.3	2.6
MS6	36	20 (S6)	28.7	4.6	1.3	1	4	1.5	0.3	2.6

A 1 mL sample of fresh mayonnaise was diluted with distilled water in a 1:2 ratio (sample: water ratio) and put on a slide without a cover glass. The sample was observed under 100x magnification at room temperature (Akhtar & Masoodi, 2022).

4.2.6.3.Texture analysis

Functional mayonnaise texture was analyzed using a TA-HD-Plus texture analyzer (Stable Micro Systems, Godalming, UK) with a 20 kg cell and 35 mm compression probe. Mayonnaise samples were placed in 35 mm tall, 54 mm diameter glass containers. A probe, inserted 8 mm deep, compressed the samples at 1 mm/s to 50% depth, measuring firmness/hardness by the highest recorded force. Consistency was assessed by the area under the curve up to the peak, cohesiveness by the greatest negative force, and the work of adhesion by the negative curve section's area.

4.2.6.4. Rheological properties

Rheological properties of the functional mayonnaise were tested using a rheometer (Model # Physical MCR 72; Make # AntonPaar, Austria) with a 25 mm diameter plate and 1 mm gap height, at 25°C. Samples were equilibrated at room temperature for 30 min before testing. Samples (approximately 2 g) were placed on the plate for analysis. Storage modulus (G') and loss modulus (G'') were assessed across angular frequencies (0.1 to 100 rad/s) in a frequency sweep test. Dynamic testing within the linear viscoelastic zone utilized a 0.5% strain amplitude. Each test was repeated twice, and average results are reported.

4.2.6.5. Oxidative stability analysis

Seven mayonnaise formulations (Control, S1, S2, S3, S4, S5, and S6) were held at 35°C for 14 days in order to test oxidative stability. The hydroperoxide production was then measured at different time intervals using the previously described method (Hosseini & Rajaei, 2020). To summarise, 8.9 mL of chloroform/methanol (3:7 v/v) was combined with 10 µL of each sample for 2–4 s. 50 µL of a 30% ammonium thiocyanate (w/v) solution was then added, and the mixture was stirred for an additional 2–4 s. Lastly, the samples were mixed with 50 µL of ferric chloride II solution. A UV–vis spectrophotometer (Agilent Technologies, Inc., Australia) was used to measure the absorbance of the

solutions at 500 nm after 20 minutes. The peroxide value (PV) is reported in millimoles of hydroperoxides per kg of oil.

4.2.6.6. RP-HPLC analysis

The β-carotene content of the samples was assessed using an RP-HPLC equipment (ThermoFisher Ultimate 3000) equipped with a UV-Vis detector and a C18 column (5 μm, 120 A, 4.6 × 250 mm). In gradient mode analysis, solvents A (methanol/acetonitrile/water 84:14:4 v/v/v) and B (100 % dichloromethane) were employed. The flow rate was 1 mL/min, the temperature was maintained at 25°C, and the wavelength was set at 450 nm. The sample extract was filtered using a 0.22 μm syringe filter before to being injected into the HPLC. Starting at 100% A and 0% B, the gradient flow programme climbed to 10% B at 4 min, 18% B at 12 min, 21% B at 17 min, and 30% B at 20 min. This was continued for 25 min, at which point it increased to 39% B at 28 min, and at the end, to 60% B at 40 min (Rohilla et al., 2023).

4.2.6.7. In-vitro lipid digestion

A simulated in-vitro gastrointestinal digestion model described by Yi et al. (2021) was used to evaluate the lipid digestion and BC bioaccessibility of functional mayonnaise.

Stomach phase: First, 0.5 g of mayonnaise dissolved in 7.5 mL of ultrapure water was mixed with 10 mL of simulated gastric fluid (SGF) containing 3.2 mg/mL pepsin and 0.15 M NaCl. The mixture's pH was then lowered to 2.0 by adding 2.5 M HCl. After that, the mixture was incubated at 37°C in a water-jacketed container while being constantly agitated at 250 rpm for an hour.

Small intestine phase: Following stomach digestion, 1M NaOH was added immediately to neutralise the liquid to pH 7.0. Next, 15 mL of simulated intestinal fluid (SIF) was added, which contained 1.0 mg/mL pancreatin, 20.0 mg/mL bile extract, and 5 mM $CaCl_2$. In a water-jacketed beaker, the intestinal digestion was carried out at 37°C while being continuously stirred at 250 rpm. 0.1 M NaOH was administered dropwise to maintain the pH at 7.0, and the amount of NaOH added was measured over the course of a 2 h intestinal digestion simulation. Using the following formula, the amount of NaOH solution added was used to determine the degree of lipolysis (%):

$$Lipolysis\ (\%) = \frac{V_{NaOH} - C_{NaOH}}{2M_{lipid}} \times 100 \qquad \textbf{Eq. 4.1}$$

Where, the volume of NaOH used is denoted by V_{NaOH}. The concentration of NaOH applied to C_{NaOH} is 0.10 M NaOH. The average molecular weight of sunflower oil (M) is known as M_{lipid}.

4.2.6.8. β-carotene bioaccessibility

The amount of β-carotene that was transferred from dispersed mayonnaise into micelles divided by the original amount of β-carotene in dispersed mayonnaise was used to calculate β-carotene bioaccessibility. After gastrointestinal digestion, the digesta was centrifuged for one hour at 10,000 rpm to produce β-carotene micelles. Next, ethanol and n-hexane (1:2, v/v) were used three times to extract β-carotene micelles. The quantity of β-carotene at 450 nm was then measured using a UV-vis spectrophotometer. Using the following formula, the bioaccessibility of β-carotene was calculated:

$$Bioaccessibility\ (\%) = \frac{amount\ of\ \beta-carotene\ \ transferred\ into\ micelles}{amount\ of\ BC\ in\ dispersed\ mayonnaise} \times 100 \qquad \textbf{Eq. 4.2}$$

4.2.7. Statistical analysis

Every experimental result is presented as a mean with standard deviations. One-way analysis of variance (ANOVA) in IBM SPSS 20.0 was used for statistical analysis. Duncan's multiple range test was used to evaluate significance levels at $p \leq 0.05$.

4.3. Results and discussion

4.3.1. Experimental design and optimization of oil phase composition

To optimize the oil phase composition, different mass ratios of sunflower oil and Tween 80 were combined at various concentrations of NC in 17 experimental runs following the BBD model (**Table 4.4**). Stable nanoemulsions with diameters < 250 nm, as determined by dynamic light scattering analysis, were successfully formed using a two-step homogenization process across all investigated oil phase compositions. RSM is a statistical technique that streamlines experimental trials by predicting outcomes based on process parameters. In this study, RSM was employed to examine the impact of oil content, Tween 80 concentration, and NC concentration on PNE. Design Expert software (Version 13.0)

facilitated regression analysis, using BBD to fit a second-order polynomial quadratic equation. The analysis of variance was used to get the regression coefficients for the linear, quadratic, and interaction variables. Visualization of the response-factor relationship and determination of optimal conditions were achieved through 3-D surface plots generated from these coefficients.

Table 4.4. Responses obtained: Particle size, PDI and Emulsion stability

Run	Experimental Factors			Responses		
	A: Oil content (%)	B: Tween 80 concentration (%)	C: Nanocellulose concentration (%)	Particle size (nm)	PDI	Emulsion stability (days)
1	5	10	2	229.5	2.821	30
2	10	7.5	3	209.6	0.145	38
3	10	7.5	1	306.5	0.465	32
4	5	7.5	3	248.2	0.756	30
5	7.5	7.5	2	209.8	1.213	42
6	7.5	7.5	2	196.4	1.636	45
7	5	7.5	1	234.6	1.898	28
8	7.5	7.5	2	191.7	1.182	44
9	7.5	7.5	2	190.8	1.547	44
10	7.5	10	1	193.7	2.821	27
11	7.5	5	1	271.17	1.782	28
12	5	5	2	246.7	0.936	21
13	7.5	10	3	200.9	1.324	32
14	10	10	2	235.6	0.198	28
15	10	5	2	281.9	2.175	37
16	7.5	7.5	2	190.5	1.282	42
17	7.5	5	3	184.31	1.822	29

The optimized response polynomial equations fitted in quadratic model for Pickering emulsion

for particle size (**Table 4.5**), PDI (**Table 4.6**), and emulsion stability (**Table 4.7**) revealed significant overall models, indicating the influence of factors on respective response variables.

Table 4.5. ANOVA of particle size for Quadratic model

Source	**Sum of Squares**	**df**	**Mean Square**	**F-value**	**p-value**	
Model	20939.21	9	2326.58	58.84	< 0.0001	**Significant** ***
A-Oil content	695.64	1	695.64	17.59	0.0041	**
B-Tween 80 concentration	1933.80	1	1933.80	48.91	0.0002	***
C-Nanocellulose concentration	3319.50	1	3319.50	83.96	< 0.0001	***
AB	211.70	1	211.70	5.35	0.0539	*
AC	3052.56	1	3052.56	77.21	< 0.0001	***
BC	2211.82	1	2211.82	55.94	0.0001	***
A^2	8486.57	1	8486.57	214.64	< 0.0001	***
B^2	248.99	1	248.99	6.30	0.0404	**
C^2	340.30	1	340.30	8.61	0.0219	**
Lack of Fit	10.51	3	3.50	0.0527	0.9819	**not significant**
R-squared	**0.9870**					
Adj R-squared	**0.9702**					

Particle size = 674.338 - 73.188 A - 34.757 B - 44 C - 1.164 AB - 11.05 AC + 9.406 BC + 7.1832 A^2 + 1.2304 B^2 + 8.99 C^2

*Significant at p<0.1, **Significant at p<0.05, ***Significant at p<0.001, df: degrees of freedom

The ANOVA table for particle size (**Table 4.5**) shows that the linear parameters - oil content, Tween 80 concentration, and nanocellulose concentration - are significant at p<0.05. The overall model is highly significant with p<0.0001. All interaction terms are

significant at $p<0.05$, except for the interaction between oil content and Tween 80 concentration (AB), which is not significant ($p>0.05$). The quadratic equation for particle size is provided in **Table 4.5.** The model's determination coefficient (R^2) is 0.9870, indicating that 98.70% of the variation in particle size is explained by the independent variables, while 1.30% remains unexplained. The lack of fit is insignificant ($p>0.05$), confirming the model's validity for optimizing particle size in Pickering nanoemulsions.

Table 4.6. ANOVA of PDI for Quadratic model

Source	**Sum of Squares**	**Df**	**Mean Square**	**F-value**	**p-value**	
Model	9.64	9	1.07	27.32	< 0.0001	**Significant** ***
A-Oil content	1.47	1	1.47	37.48	0.0005	***
B-Tween 80 concentration	0.0252	1	0.0252	0.6430	0.4490	
C-Nanocellulose concentration	1.07	1	1.07	27.18	0.0012	**
AB	3.73	1	3.73	95.14	< 0.0001	***
AC	0.1689	1	0.1689	4.31	0.0765	*
BC	0.5906	1	0.5906	15.07	0.0060	**
A^2	0.9716	1	0.9716	24.79	0.0016	**
B^2	1.73	1	1.73	44.13	0.0003	***
C^2	0.0241	1	0.0241	0.6144	0.4588	
Lack of Fit	0.1045	3	0.0348	0.8209	0.5464	**not significant**
R-squared	**0.9723**					
Adj R-squared	**0.9367**					

PDI = -5.40113 + 1.9757 A - 0.04965 B + 0.473875 C - 0.15448 AB + 0.0822 AC - 0.1537 BC - 0.07686 A^2 + 0.10254 B^2 - 0.075625 C^2

*Significant at $p<0.1$, **Significant at $p<0.05$, ***Significant at $p<0.001$, df: degrees of freedom

The ANOVA table for PDI (**Table 4.6**) shows that the linear parameters - oil content and nanocellulose concentration - are significant at $p<0.05$, while Tween 80 concentration is non-significant. The overall model is highly significant with $p<0.0001$. All interaction terms are significant at $p<0.05$, except for the interaction between oil content and nanocellulose concentration (AC), which is not significant ($p>0.05$). The quadratic equation for PDI is presented in **Table 4.6.** The determination coefficient (R^2) is 0.9723, indicating that 97.23% of the variation in PDI is explained by the independent variables, while 2.77% remains unexplained. The lack of fit is insignificant ($p>0.05$), validating the model for optimizing PDI in Pickering nanoemulsions.

Table 4.7. ANOVA of emulsion stability for Quadratic model

Source	**Sum of Squares**	**Df**	**Mean Square**	**F-value**	**p-value**	
Model	856.24	9	95.14	76.55	< 0.0001	**Significant** ***
A-Oil content	84.50	1	84.50	67.99	< 0.0001	***
B-Tween 80 concentration	0.5000	1	0.5000	0.4023	0.5461	
C-Nanocellulose concentration	24.50	1	24.50	19.71	0.0030	**
AB	81.00	1	81.00	65.17	< 0.0001	***
AC	4.00	1	4.00	3.22	0.1159	
BC	4.00	1	4.00	3.22	0.1159	
A^2	136.80	1	136.80	110.07	< 0.0001	***
B^2	318.69	1	318.69	256.42	< 0.0001	***
C^2	136.80	1	136.80	110.07	< 0.0001	***
Lack of Fit	1.50	3	0.5000	0.2778	0.8395	**not significant**
R-squared	**0.9899**					
Adj R-squared	**0.9770**					
Emulsion stability = -151.5 + 19.58 A + 25.58 B + 18.55 C - 0.72 AB + 0.4 AC + 0.4 BC - 0.912 A^2 - 1.392 B^2 - 5.7 C^2						

*Significant at $p<0.1$, **Significant at $p<0.05$, ***Significant at $p<0.001$, df: degrees of freedom

The ANOVA table for emulsion stability (**Table 4.7**) shows that the linear parameters - oil content and nanocellulose concentration - are significant at $p<0.05$, while Tween 80 concentration is non-significant. The overall model is highly significant with $p<0.0001$. The interaction between oil content and Tween 80 concentration is significant at $p<0.05$, but the interactions between oil and nanocellulose (AC) and Tween 80 and nanocellulose (BC) are not significant ($p>0.05$). The quadratic equation for emulsion stability is provided in **Table 4.7.** The determination coefficient (R^2) is 0.9899, indicating that 98.99% of the variation in emulsion stability is explained by the independent variables, with 1.01% unexplained. The lack of fit is insignificant ($p>0.05$), confirming that the model is valid and reliable for optimizing emulsion stability in Pickering nanoemulsions.

Overall, the models demonstrated significant impact of oil, Tween 80, and nanocellulose concentrations on particle size, with nanocellulose concentration being the most influential. In PDI optimization, oil content stood out as the significant factor, while for particle size, nanocellulose concentration played a crucial role. Previous research has demonstrated that emulsifier structures resembling those of biopolymer emulsifiers may facilitate the formation of stable emulsified states in smaller droplets (Poncelet et al., 1995). In conclusion, these analyses underscore the importance of considering oil, Tween 80, and nanocellulose concentrations in optimizing particle size, with oil content being particularly crucial for PDI optimization. Nanocellulose concentration is pivotal for achieving emulsion stability. Studies have revealed that the particle size of emulsion decreases as nanoparticle concentration increases (Tan et al., 2014; Li et al., 2018). Therefore, the models fit the data well and explain a substantial portion of the variability observed in each optimization process, providing valuable insights for further refinement and application in food emulsions.

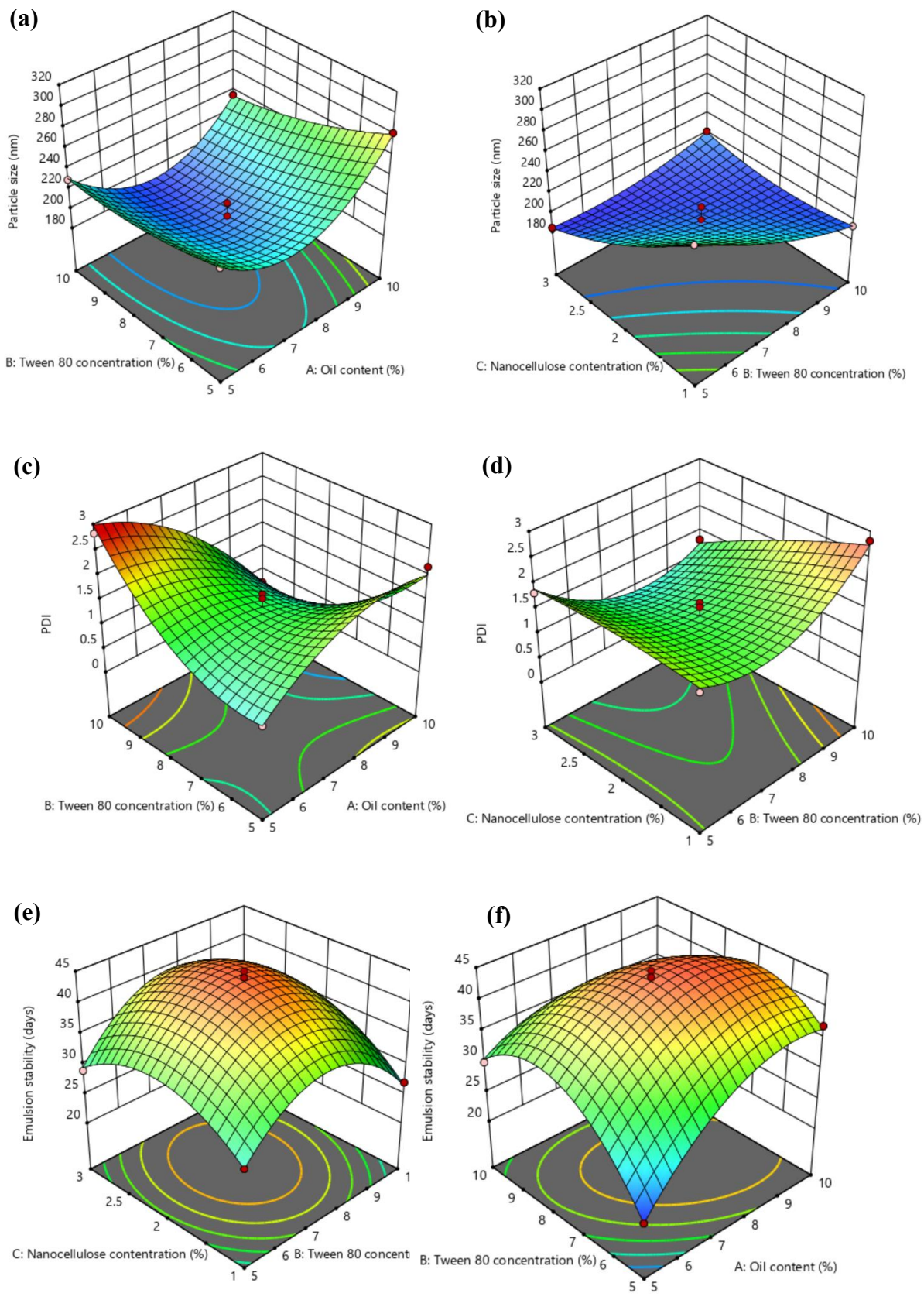

Fig. 4.1. 3D surface graphs: (a, b) particle size, (c, d) PDI, and (e-f) emulsion stability.

The interactive effects of independent variables on particle size, PDI, and emulsion stability were analysed using three-dimensional response surface profiles. Oil content, Tween 80 concentration, and nanocellulose concentration were varied, and their effects on dependent variables were visualized through 3D surface graphs (**Fig. 4.1**). In **Fig. 4.1. (a, b)**, particle size initially decreased with increasing oil content and Tween 80 concentration but later increased with its increased concentration. For PDI, dispersibility decreased with increasing oil content and Tween 80 concentration. Also, dispersibility initially decreases and then increases if we increase the nanocellulose and Tween 80 concentration as shown in **Fig. 4.1. (c, d)**. Emulsion stability initially increased and then decreased with increasing nanocellulose concentration and Tween 80 concentration. Additionally, emulsion stability initially increased with increasing oil content and Tween 80 concentration but later exhibited a reverse trend which can be seen at **Fig. 4.1. (e-f).**

Table 4.8. Optimum conditions, experimental and predicted values

Independent variables	**Coded Levels**	**Actual Levels**	
Oil content (%)	-0.038	7.405	
Tween 80 concentration (%)	0.338	8.344	
Nanocellulose Concentration (%)	0.352	2.352	
Responses	**Predicted Values**	**Experimental Values**	**Desirability**
Particle size (nm)	200.12	**204.5**	1
PDI	1.543	**1.722**	
Emulsion stability (days)	38	**35**	

$$\mathbf{Z=(Z_0-Z_c)/\Delta Z}$$

Where, Z and Z_0 indicate coded and actual levels of independent variables, respectively. ΔZ represents step change while Z_c indicated actual value at central point.

The process was validated based on desirability (**Table 4.8**), yielding the highest desirability of 1 at the following optimal conditions- oil content: 7.405%, Tween 80 concentration: 8.344%, and nanocellulose concentration: 2.352%. Predicted values for particle size was 200.12 nm, PDI was 1.543, and emulsion stability was 38 days.

Experimental values obtained for particle size was 204.5 nm, PDI was 1.722, and emulsion stability was 35 days. DLS data (**Fig. 4.2**) supported the experimental values, indicating minimal deviation from predicted values and validating the chosen conditions for further study.

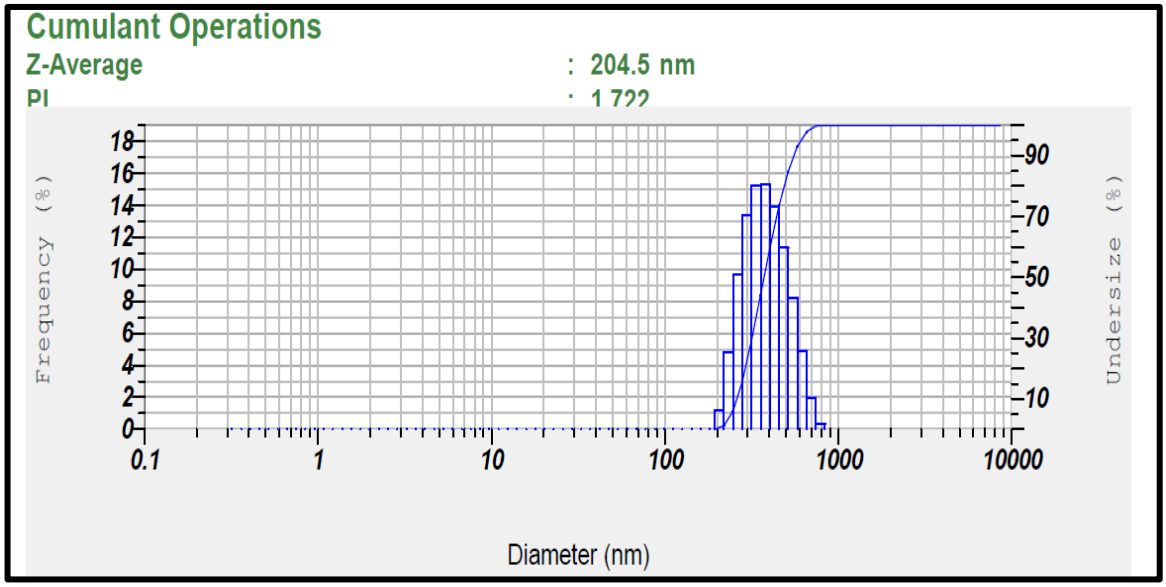

Fig. 4.2. Particle size analysis of optimized Pickering nanoemulsion.

4.3.2. Characterisation of Pickering nanoemulsion

4.3.2.1. Emulsion stability during storage

PNE was generated for the storage study utilising the optimised conditions reported in **section 4.3.1. Fig. 4.3** depicts digital photographs of nanoemulsion stabilized with BRNC on days 0 and 35, showcasing visual similarity and absence of phase separation initially, thus maintaining physical stability over the 35-day storage period. The fresh samples exhibited robust stability against coalescence, sedimentation, and creaming conditions. Initially, all fresh emulsions appeared opaque, homogeneous, and single-phased in accordance with a reported study of Meirelles et al. (2020). Solid fine particles exhibit significant potential as stabilizing agents in Pickering emulsions. Because of their high adsorption energy, these particles, in contrast to surfactant molecules, adsorb at liquid/liquid interfaces irreversibly. As a result, Pickering emulsions typically offer enhanced stability compared to surfactant-stabilized systems, presenting extensive versatility in material processing (Fujisawa et al., 2017).

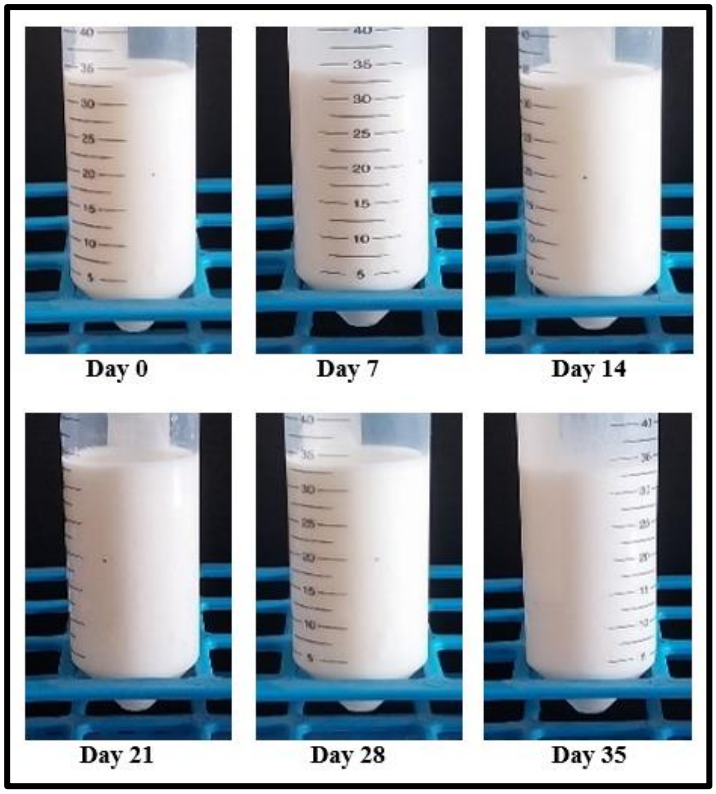

Fig. 4.3. Physical stability check of optimized emulsion during storage at 25°C for 35 days.

Unstable emulsions typically undergo phase separation, manifested as distinct layers of aqueous and oil phases with an emulsified intermediate phase. However, our developed emulsions remained visually stable and retained their homogeneous and single-phase characteristics during the study duration, with no observable significant changes in particle aggregation within the colloidal system. According to Bai et al. (2019), there are three main mechanisms responsible for the remarkable long-term stability of nanocellulose in the form of cellulose nanocrystals (CNC)-based Pickering emulsions: (1) strong electrostatic repulsion due to the high surface potential of CNC-coated oil droplets; (2) significant steric repulsion aided by the formation of a dense CNC assembly encasing the droplet surfaces; and (3) the irreversible adsorption of CNCs onto the oil droplet surfaces, a feature of Pickering stabilisation. Furthermore, the achieved stability is influenced by the viscosity of the oils and the interphase formed between water and oil, which collectively hinder oil droplet coalescence. Additionally, the formation of a robust nanocellulose-based three-dimensional network within the emulsion further contributes to its stability (Souza et al., 2020). The stability of an emulsion is due to its capacity to hold onto its characteristics during storage.

4.3.2.2. Particle size analysis

The particle size distribution of the optimized PNE was monitored over a 35-day period, with measurements taken at 7-day intervals**. Fig. 4.4.** illustrates the average particle size recorded on various days throughout 35 days of storage. No significant difference in the size of the particles were observed till day 14 of storage indicating that no droplet coalescence occurred during storage except a slight increase in the later days of storage (from day 21 to day 35). This outcome is likely due to the hydrophobic nature of sunflower oil, which modified the balance between hydrophobicity and hydrophilicity in the nanoemulsion. These findings align with previous research (R. S. Hosseini & Rajaei, 2020).

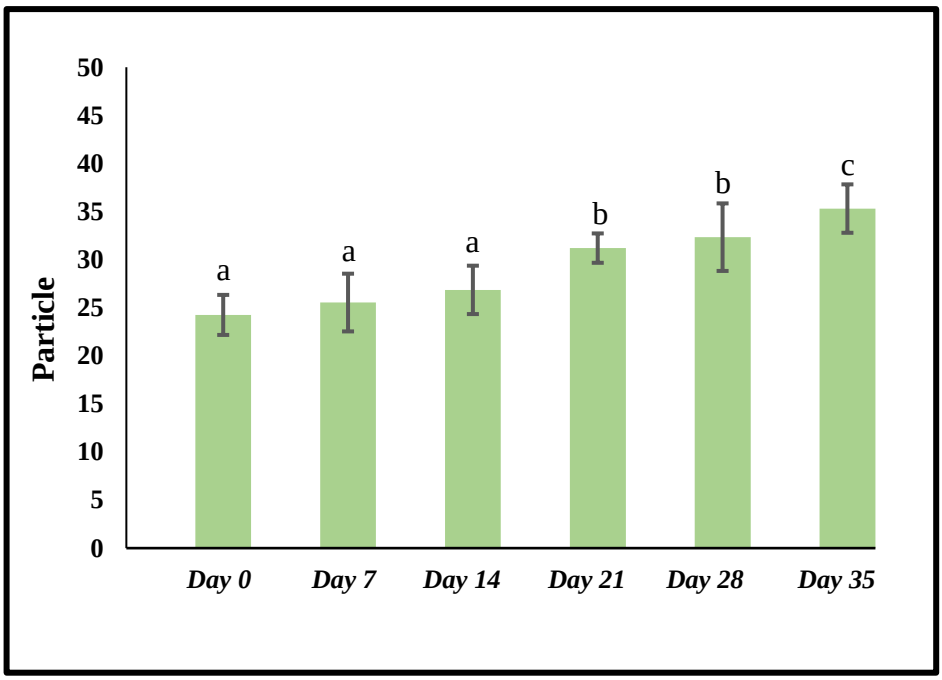

Fig. 4.4. Particle size of optimized Pickering emulsion for a period of 35 days.

Despite a slight change in particle size, the emulsion remained stable throughout the 35-day storage period, with no occurrence of phase separation. At an adequate concentration of NC, a three-dimensional network is formed, aiding in the stabilization of the emulsion and preventing coalescence of oil droplets (Rayner et. al.,2014; Gao et. al., 2017; Li et al., 2018). The average of initial particle size of the freshly prepared PNE (day 0) was 196.2 nm. Throughout the observation period, spanning from 7 to14 days, the particle size remained comparable to those of day 0, with no statistically significant difference. From

day 21 onwards, the average particle size significantly increased to an average particle size of 248 nm on day 35. The observed increase in particle size suggests a potential interaction between the nanocellulose-based particle stabilizer and the oil droplet surfaces. However, this mechanism may also account for the slight changes observed in particle size over the storage period.

4.3.2.3. Morphological analysis

Fig. 4.5. displays the changes in the microscopic structure of PNE stabilized with nanocellulose on storage for different days. Over a period of 35 days, optical microscopic pictures were taken at room temperature once every seven days. The images revealed uniformly distributed small sized spherical droplets. Larger droplets that were observed appeared to remain separate. According to Chen et al. (2019), this separation does not indicate a trend of flocculation but rather signifies the stability of the emulsion. The presence of larger droplets in the emulsion suggests a balance where insufficient energy prevents all droplets from breaking down into smaller ones, thereby enhancing the stability of the emulsion. This stability, which keeps the droplets separated, is attributed to electrostatic forces resulting from the nanocellulose coating on the oil droplets. These forces cause repulsion between droplets due to the negative charges generated by the nanocellulose's free hydroxyl groups (Souza et al., 2021). The observed increase in droplet size from 196.2 nm to 248 nm (**Fig. 4.4**) over the storage period of 35 days suggested that nanocellulose may have adsorbed onto the droplet surfaces and entangled to form a network structure, that protected the droplets from flocculation (Ni et al., 2020).

Day 0

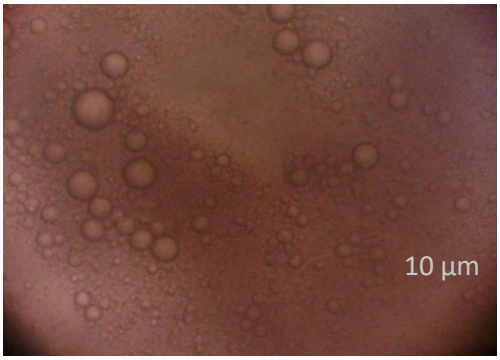

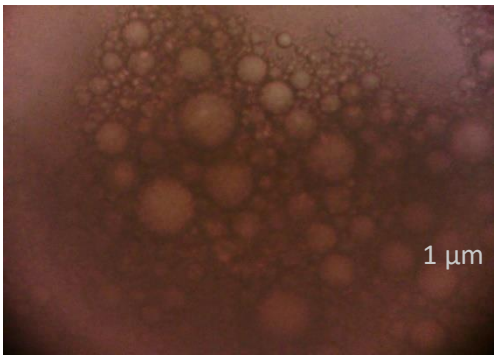

Day 7

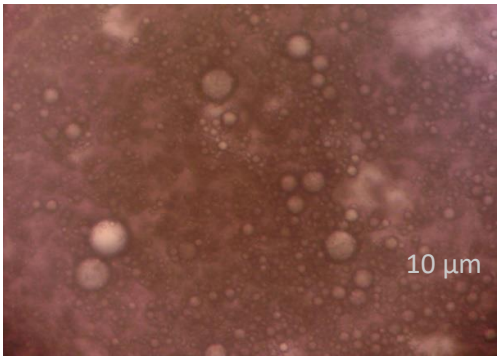

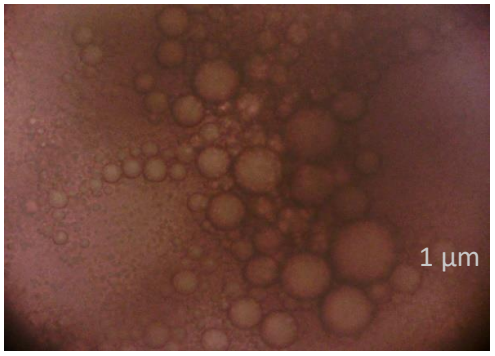

Day 14

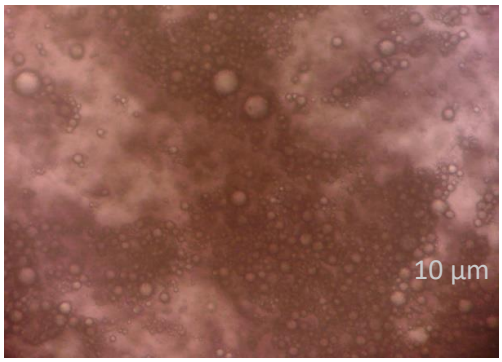

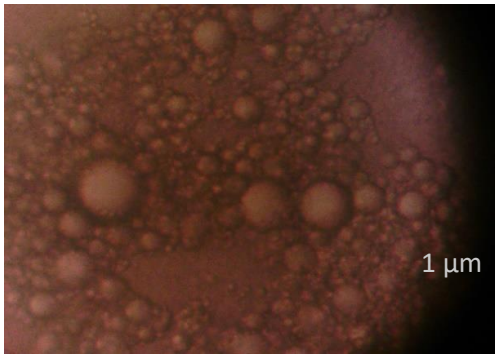

Day 21

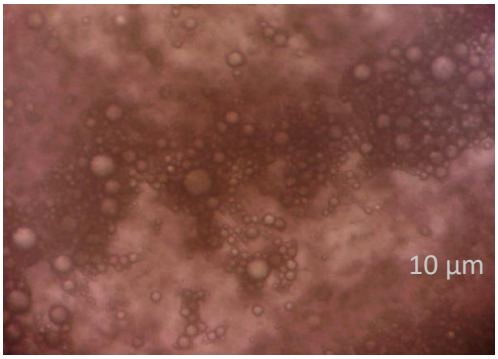

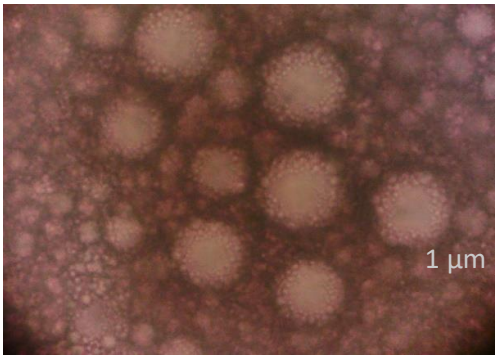

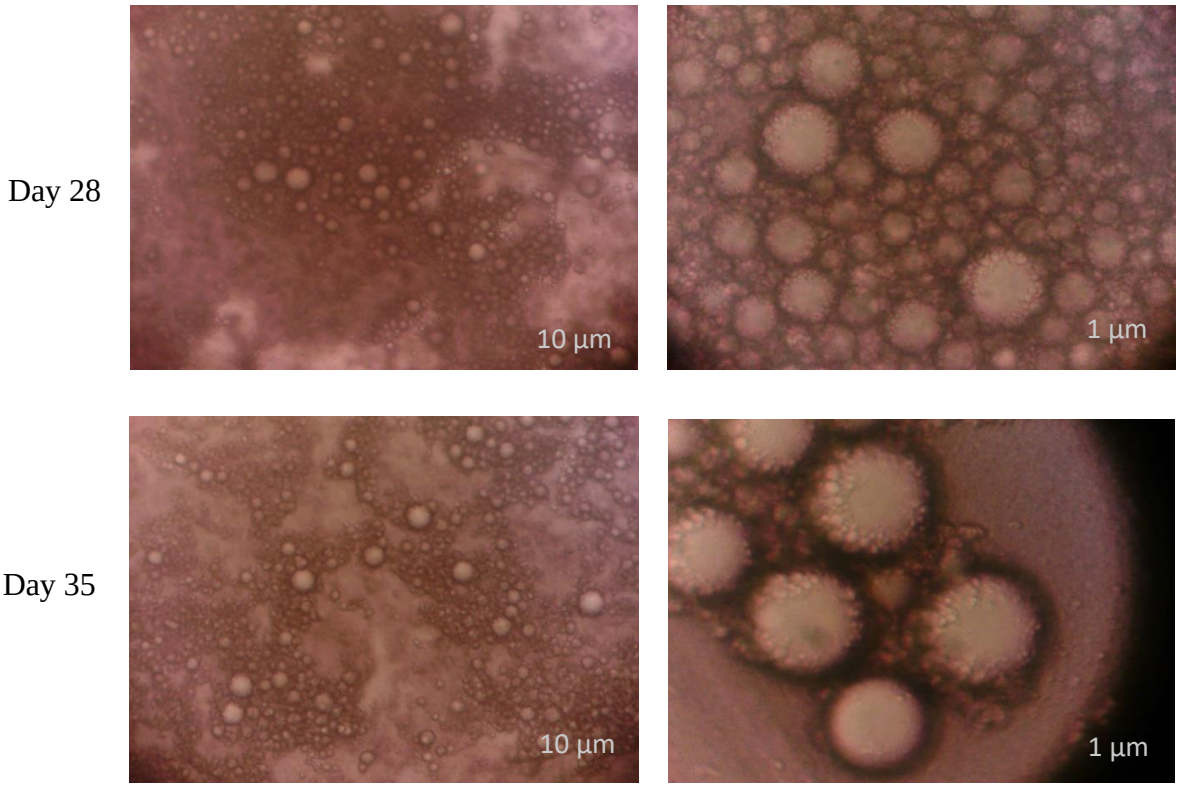

Fig. 4.5. Optical microscopy images of Pickering nanoemulsion (PNE) stabilized with nanocellulose in optimized processing parameters obtained at 7 days interval during storage at RT (28°C) for 35 days.

4.3.3. Chemical stability of β-carotene encapsulated Pickering nanoemulsion

The impact of the developed PNE on β-carotene chemical stability was investigated. **Fig. 4.6**. presents the degradation curves of β-carotene in ethanol solution (control) and β-carotene entrapped in PNE after exposure to UV radiation. The control represents β-carotene (0.02 g/10 mL) in ethanol solution, while samples S1 to S6 denote varying concentrations of β-carotene present in PNE. UV light exposure significantly reduced β-carotene's stability in ethanol solution, with rapid degradation observed over time. Conversely, the PNE method significantly increased the photostability of β-carotene (Xia et al., 2022). Even after exposure to UV light for 8 h, β-carotene nanoemulsion droplets maintained their color, with a retention rate of 0.81 for sample S6, surpassing that of β-carotene in ethanol solution (0.48).

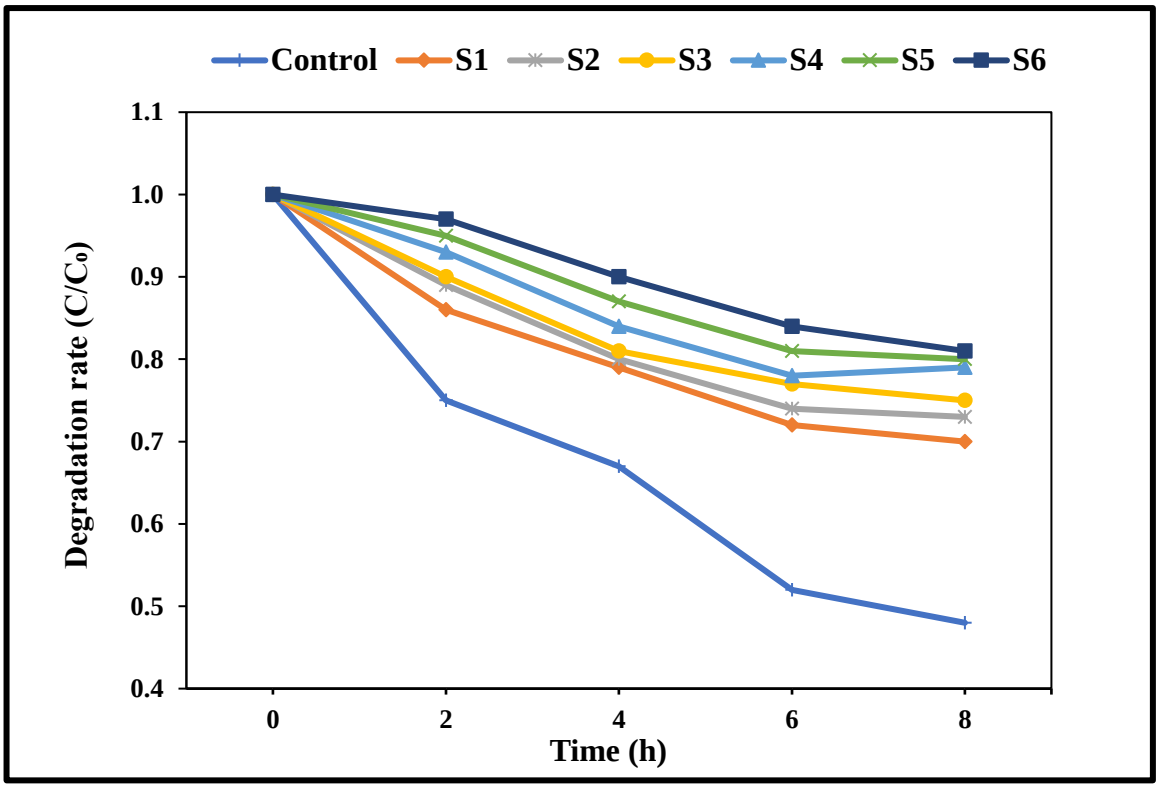

Fig. 4.6. Degradation curve of β-carotene in ethanol solution (control) and in PNEs under UV-light (C is the content of β-carotene after storage for a period t against UV light, while C_0 is the initial β-carotene content at preparation of stabilized β-carotene-loaded Pickering emulsions).

Furthermore, retention rate increased with an increase in the concentration of β-carotene. The increased stability has been ascribed to the nanocellulose particles creating an interface membrane that successfully restricted the penetration of light and oxygen through the β-carotene droplets' outer shell. This mechanism significantly enhanced the stability of β-carotene against UV light-induced degradation, highlighting the efficacy of the PNE technique in preserving the functional properties of β-carotene (Wei & Gao, 2016).

4.3.4. Characterisation of functional mayonnaise

4.3.4.1. Color analysis, stability, and visual appearance of functional mayonnaise

The prepared mayonnaise samples underwent color analysis (Table 7) using *L**, *a**, and *b** parameters at various periods of storage (day 1, 7, and 14) to examine any change in color. The *L**, *a** and *b** values in **Table 4.9.** suggested that control sample had the highest

lightness, lowest redness and yellowness values when compared to the mayonnaise samples (MS1-MS6). The addition of β-carotene encapsulated PNE to the functional mayonnaise resulted in significant ($p < 0.05$) color changes in the samples, given that the mayonnaise initially had an orange color that intensified with the concentration of the nanoemulsion added. As the amount of emulsion that was added increased during mayonnaise manufacture, the lightness of the mayonnaise (L^* values) decreased significantly ($p < 0.05$) across samples and across days of storage. Similarly, a^* and b^* values increased significantly across samples and across days of storage. a^* values changed from 1.50-6.90 in MS1-MS6 on day 1 to 2.05-7.91 on day 14. At the same time, b^* values changed from 12.13-24.23 in MS1-MS6 on day 1 to 13.31-26.18 on day 14. Similar effect was also reported by Blejan and Nour (2023).

It can be stated that the addition of β-carotene encapsulated PNE led to a significant reduction in lightness of samples across MS1-MS6 and enhancement of the redness and yellowness values, which can be attributed to the higher β-carotene concentration. Thus, the incorporated β-carotene was retained in the mayonnaise sample, which increased its functional properties. The technique of incorporating bioactive compounds in PNE has shown to be a perfect way to improve the stability of mayonnaise and create a functional mayonnaise. The unique orange-red color of mayonnaise samples (MS1-MS6) is attributed to the presence of parent carotenoids (Haniff et al., 2020), with color changes possibly intensified by chemical interactions and exposure to oxygen within the container, leading to oxidation-induced complex color alterations as observed with organic chemicals in food when subjected to air and heat.

Different concentrations of β-carotene were added to mayonnaise to develop a functional product, as depicted in **Fig. 4.7.** This addition aimed to increase the concentration of β-carotene within the mayonnaise to enhance its functional properties. Increasing the concentration of β-carotene is expected to enhance its functional properties, such as antioxidant activity or color intensity, thereby potentially improving the nutritional profile and visual appeal of the mayonnaise.

Table 4.9. Colour analysis of functional mayonnaise samples fortified with encapsulated β-carotene over extended storage periods

		Control	**MS1**	**MS2**	**MS3**	**MS4**	**MS5**	**MS6**
Day1	**L***	73.93 ± 0.59^{aA}	71.76 ± 0.21^{bA}	69.36 ± 0.37^{cA}	68.68 ± 0.10^{cA}	66.30 ± 0.05^{eA}	66.43 ± 0.27^{dA}	66.45 ± 0.57^{cA}
	a*	0.13 ± 0.01^{fC}	1.50 ± 0.11^{eB}	3.89 ± 0.23^{dAB}	5.19 ± 0.05^{bA}	4.72 ± 0.06^{cC}	5.46 ± 0.13^{bC}	6.90 ± 0.33^{aC}
	b*	9.54 ± 0.09^{gC}	12.13 ± 0.22^{fC}	17.89 ± 0.17^{eA}	19.65 ± 0.04^{cC}	18.84 ± 0.08^{dC}	20.33 ± 0.21^{bC}	24.23 ± 0.29^{aC}
Day7	**L***	73.30 ± 0.06^{aA}	71.37 ± 0.12^{bB}	68.54 ± 0.11^{cAB}	67.99 ± 0.09^{dB}	65.79 ± 0.02^{gB}	67.48 ± 0.06^{eA}	66.50 ± 0.02^{fA}
	a*	0.35 ± 0.04^{gB}	2.11 ± 0.02^{fA}	4.15 ± 0.01^{eA}	5.19 ± 0.03^{dA}	5.35 ± 0.01^{cB}	6.18 ± 0.01^{bB}	7.69 ± 0.01^{aA}
	b*	9.75 ± 0.10^{gB}	13.63 ± 0.04^{fA}	18.91 ± 0.05^{eA}	20.58 ± 0.15^{cB}	20.06 ± 0.02^{dB}	21.50 ± 0.13^{bB}	25.74 ± 0.01^{aB}
Day14	**L***	72.08 ± 0.19^{aB}	70.94 ± 0.09^{aC}	66.16 ± 2.18^{bcB}	66.88 ± 0.15^{bC}	64.78 ± 0.11^{cC}	66.35 ± 0.17^{bcB}	65.87 ± 0.16^{bcA}
	a*	0.45 ± 0.00^{gA}	2.05 ± 0.04^{fA}	3.66 ± 0.06^{eB}	5.07 ± 0.08^{dB}	5.61 ± 0.05^{cA}	6.53 ± 0.09^{bA}	7.91 ± 0.03^{aA}
	b*	10.01 ± 0.11^{fA}	13.31 ± 0.04^{eB}	18.62 ± 0.89^{dA}	21.26 ± 0.05^{cA}	20.81 ± 0.11^{cA}	22.47 ± 0.26^{bA}	26.18 ± 0.01^{aA}

*Small superscript represents significant difference ($p<0.05$) between columns but within same row and capital superscript represents significant difference ($p<0.05$) between rows but within same column.

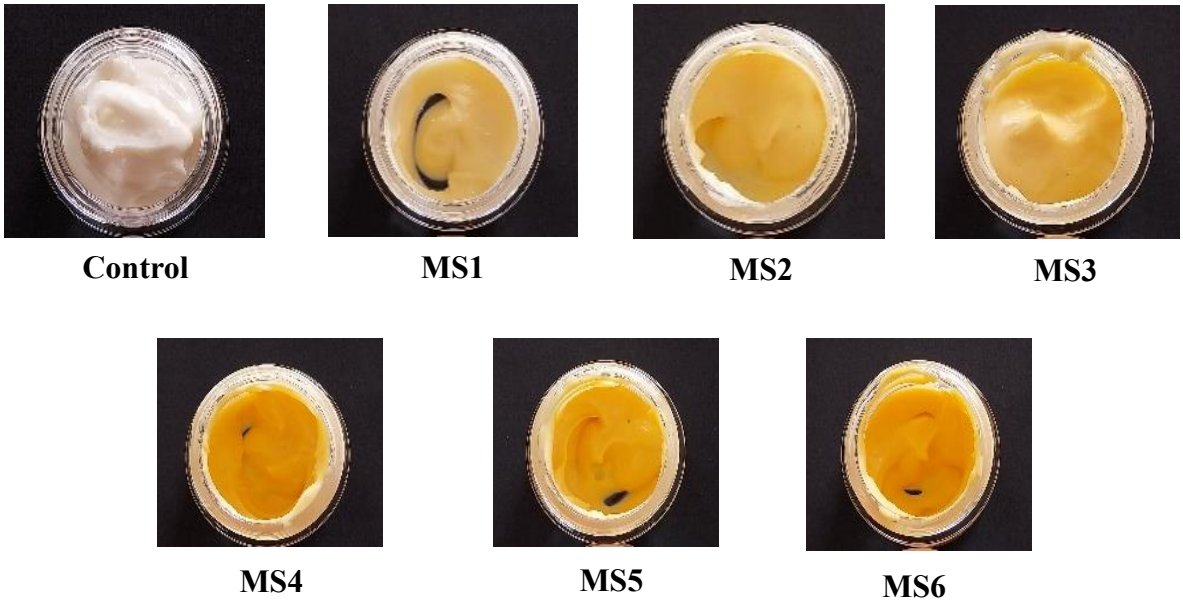

Fig. 4.7. Appearance of functional mayonnaise enriched with Pickering nanoemulsions loaded with β-carotene.

Figure 4.7. illustrates the images of β-carotene encapsulated PNE-enriched mayonnaise samples at varying concentrations. The freshly prepared mayonnaise exhibited a self-standing gel, with the control displaying a whitish hue, while increasing emulsion concentration led to observable color changes. Color parameters were analysed and recorded in **Table 4.9** to document these changes accurately. Visually, the control sample displayed a firm gel without phase separation or creaming, attributed to its three-dimensional complex network. Mayonnaise samples (MS1-MS6) were expected to exhibit a characteristic non-Newtonian fluid behaviour, limiting the free movement of oil droplets, a property influenced by the primary three-dimensional network structures of PNE due to particle interaction on droplet surfaces (Akhtar & Masoodi, 2022). Increasing PNE concentration facilitated layer-by-layer deposition of β-carotene and nanocellulose, ensured full coverage of oil globules and resulted in the generation of smaller oil droplets during the emulsification process (Fitri et al., 2022). Increased adsorption of the nanoemulsion enhanced mayonnaise stabilization by inhibiting droplet aggregation through heightened electro-steric repulsions. The addition of β-carotene and nanocellulose improved emulsifying capacity, which can be attributed to fibril bundles formation entangling the particles, thus enhancing emulsification during shear-induced processes (Akcicek et al., 2022).

4.3.4.2. Optical microscopic analysis of functional mayonnaise

Figure 4.8. presents the optical images of mayonnaise samples enriched with β-carotene encapsulated PNE. All mayonnaise samples showed spherical droplets and with increase in the PNE concentration, the increase in the concentration of the nanocellulose particle can be seen in the images. MS6 sample showed the highest concentration of nanoparticles. The emulsion droplets progressively became more uniform as the solid contents increased due to the adsorption of increasingly complex particles at the oil-water interface caused by the incorporation of β-carotene encapsulated PNE with increasing nanocellulose concentration (MS1-MS6). The emulsion droplets interact with one another due to the presence of the nanoparticles, forming a gelled condition that inhibits coalescence. Phase separation is delayed as a result of the greater phase viscosity and decreased oil droplet mobility brought on by the higher concentration of these particles (Akhtar & Masoodi, 2022). As seen in the figure, the interaction between the complex particle and the emulsion droplets managed to create a stable oil dispersion that prevented coalescence and flocculation of the oil droplets. Thus, our findings implied that adding nanoparticles to mayonnaise could enhance its microstructural qualities.

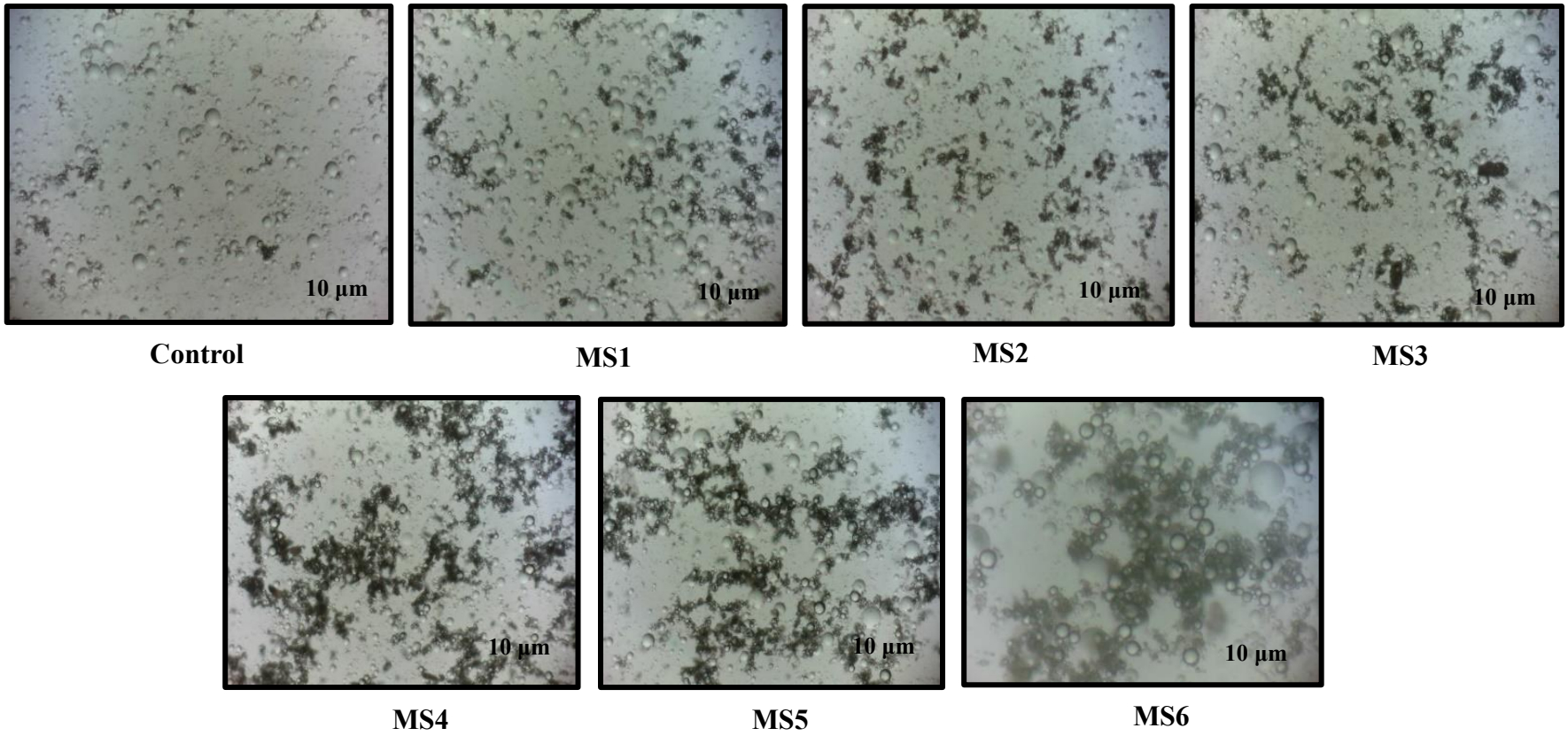

Fig. 4.8. Optical microscopic images of mayonnaise enriched with Pickering nanoemulsions loaded with β-carotene.

4.3.4.3. Texture analysis of functional mayonnaise

As indicated by the data presented in **Table 4.10**, significant variations ($p > 0.05$) in characteristics of texture (hardness, gumminess, cohesiveness, springiness, and adhesiveness) were observed among the samples (Control and MS1-MS6). The force required to compress the sample to a particular degree of deformation is represented by hardness, which stands for firmness, whereas springiness shows how easily the food system returns to its initial shape once the applied force is removed. Adhesiveness refers to the tendency of a material to stick to other surfaces. That means it represents how sticky or adhesive the samples are to the given surface. Cohesiveness reflects the degree of deformation of the sample before fracture and is a secondary parameter in texture profile analysis, while gumminess, calculated by multiplying hardness with cohesiveness, is another secondary TPA parameter. Hardness is a crucial textural attribute that impacts both mouthfeel and the processability of the product (Chang et al., 2017). The highest hardness or firmness value was found in the MS6 mayonnaise sample followed by the other samples like MS5, MS3, MS4, MS2, MS1 and control. The increase in the hardness value might be due to the addition of the β-carotene encapsulated PNE added in different concentrations. The incorporation of encapsulated PNE resulted in increased firmness compared to the control sample, which can be attributed to the presence of stabilizing compounds in the added PNE, particularly nanocellulose. Nanocellulose's ability to stabilize both oil and water reduces the fluidity of the functional mayonnaise, leading to a more compact oil-in-water structure and a uniform texture, thereby enhancing the hardness and adhesiveness of the functional mayonnaise (Wang et al., 2022). The adhesiveness values seem to vary among different samples, with the MS6 sample having the maximum mean adhesiveness value of -994.234 ± 0.106. It was also observed that both springiness and gumminess increased parallelly after the addition of PNE even though the trend was not obvious. Furthermore, the addition of β-carotene encapsulated PNE in the composition of mayonnaise improved cohesiveness as well, giving the product a delicate and acceptable texture.

Table 4.10. Texture analysis of functional mayonnaise samples

	Hardness (g)	Adhesiveness (g.sec)	Springiness	Cohesiveness	Gumminess
Control	250.886±0.413^{f}	-722.756±0.219^{b}	0.951±0.017^{abc}	0.573±0.002^{ab}	150.656±0.219^{f}
MS1	262.942±0.296^{e}	-844.667±0.703^{d}	0.941±0.008^{bc}	0.582±0.009^{ab}	168.666±0.646^{c}
MS2	285.337±0.947^{d}	-657.438±0.915^{a}	0.928±0.184^{c}	0.562±0.002^{bc}	167.551±0.877^{d}
MS3	290.097±0.374^{c}	-884.672±0.679^{e}	0.931±0.176^{c}	0.594±0.019^{ab}	174.519±0.539^{b}
MS4	285.098±0.236^{d}	-770.920±0.665^{c}	0.962±0.021^{ab}	0.535±0.003^{c}	152.560±0.519^{e}
MS5	292.333±0.701^{b}	-964.234±1.624^{f}	0.963±0.117^{ab}	0.568±0.025^{abc}	143.807±0.554^{g}
MS6	348.072±0.386^{a}	-994.242±0.106^{g}	0.973±0.008^{a}	0.601±0.405^{a}	196.557±0.106^{a}

Average of mean values ± standard deviation means values. Means in a column followed by different letters are significantly different ($P < 0.05$).

4.3.4.4. Oxidative stability of functional mayonnaise

Lipid oxidation significantly impacts the degradation of commercial food emulsions, leading to compromised quality, notably in terms of sensory attributes like undesirable rancidity and the formation of potentially harmful compounds. This degradation primarily arises from the generation of primary and secondary compounds, including peroxides, aldehydes, and ketones (Ghirro et al., 2022; Song et al., 2020). The oxidative stability of mayonnaise, with or without β-carotene enrichment, was evaluated over a 14-day period by monitoring hydroperoxide levels (**Fig. 4.9**). The trend showed an increase in hydroperoxide formation in the control group up to day 14. However, there were no significant differences ($p > 0.05$) observed among the various treatments on day 1 and day 7 of storage. Additionally, no significant differences ($p > 0.05$) were noted in hydroperoxide formation across MS1–MS6 samples until the 14th day of analysis. The incorporation of β-carotene encapsulated emulsion significantly inhibited the production of hydroperoxides in mayonnaise. The development of a thick protective layer surrounding the β-carotene droplets may be the cause of this decrease in oxidation rate, effectively preventing contact between the oil and peroxidants. Protecting against oxidative damage, β-carotene's unsaturated structure and aromatic carotenoid rings may help neutralise free radicals and singlet oxygen (Akcicek et al., 2022).

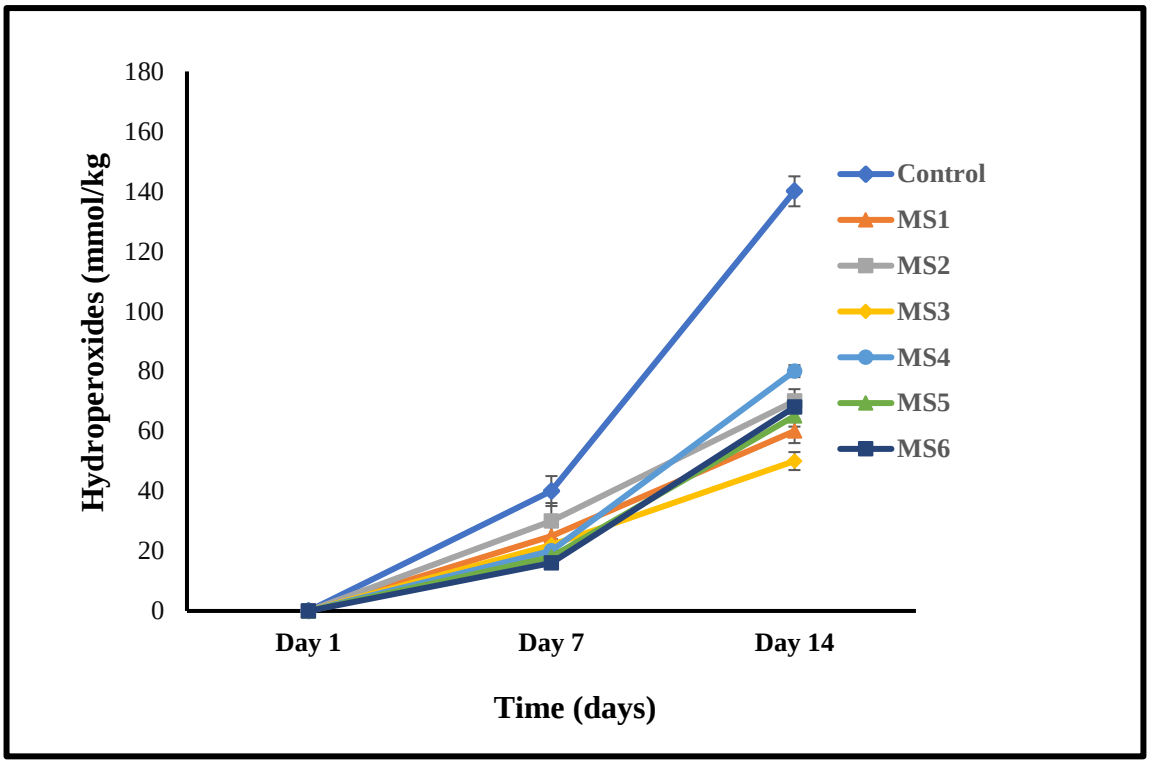

Fig. 4.9. Amount of hydroperoxides in mayonnaise samples fortified with β-carotene during 14 days of storage at 4°C.

In oil-in-water emulsions, the composition and structure of the oil-water interface play a crucial role in regulating the rate and extent of lipid oxidation (Borel et al., 2014). β-carotene, combined with nanocellulose, exhibits specific radical scavenging properties through hydrogen transfer, and thereby terminates radical chain reactions in heterogeneous systems (Akhtar & Masoodi, 2022; Yuan et al., 2017). Particles derived from compounds with antioxidant properties, such as curcumin, have been demonstrated to enhance the inhibition of peroxidants, thus improving the oxidative stability of emulsions (Mwangi et al., 2020). Furthermore, microcrystalline cellulose particles utilized to stabilize Pickering emulsions were found to reduce the rate of lipid oxidation (Kargar et al., 2012a). As a result, the developed mayonnaise samples exhibited significantly enhanced oxidative stability compared to the control, indicating increased resistance to peroxidation by-products and potentially extending the product's shelf life. The synergistic effects on oxidative stability that the combination of antioxidant β-carotene enrichment and PNE-based encapsulation technique demonstrated improved shelf life of mayonnaise.

4.3.4.5. Rheological properties of functional mayonnaise

Fig. 4.10. illustrates the samples of mayonnaise supplemented with β-carotene and their storage modulus (G') and loss modulus (G"). It is evident that at low frequencies across all samples, G' exceeded G", indicating the dominance of elastic behaviour over viscous behaviour, and thus a gel-like consistency existed. However, the viscous behaviour surpassed the elastic behaviour at higher frequencies. This finding implied that weak intermolecular force was the main cause of the gel shape in the samples, as evidenced by their breakage at high frequencies (Hosseini & Rajaei, 2020).

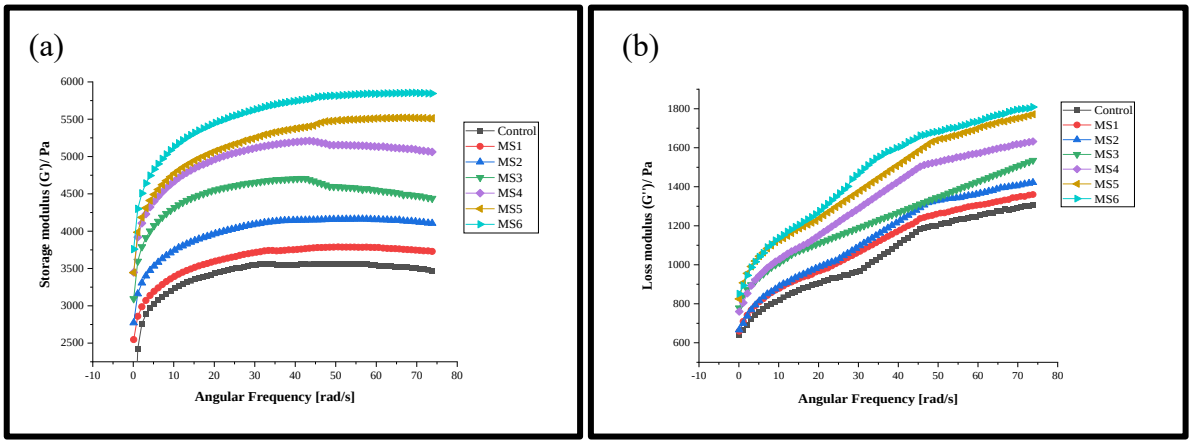

Fig. 4.10. (a): Storage modulus (G') and (b): loss modulus (G") values (in log) against angular frequency of mayonnaise products enriched with Pickering nanoemulsions loaded with β-carotene.

However, despite the weak intermolecular forces, over the frequency range, there was no crossover of G' and G" because the network created by each gel held together even at higher angular frequencies. Thus, the gels did not change into viscous liquids and retained their viscoelastic characteristics over the frequency sweep. Higher frequency values show a rising trend in the G' and G" modulus, which suggests a strong gel structure. Because of the high molecular weight β-carotene's involvement in both covalent and non-covalent interactions, the restricted mobility of nanocellulose particles adsorbed onto the oil droplet surfaces is the reason for the mayonnaise's higher G' values. These gels, often termed emulgels, exhibit solid-like behavior with high viscosity and storage modulus (G') surpassing the loss modulus (G") at low strains. Our observations are consistent with previous findings (Akhtar & Masoodi, 2022). According to Huang et al. (2016), the

network formation among lipoproteins adsorbed surrounding nearby oil droplets is also responsible for mayonnaise's viscoelastic characteristics.

Table 4.11. Power law model parameters of mayonnaise samples

Samples	**β-carotene concentration (mg)**	**K (Pa s^n)**	**n**	**R^2**
Control	0	$670.01 \pm 0.75_g$	0.31 ± 0.0002	0.95
MS1	20	$709.11 \pm 0.04_e$	0.10 ± 0.02	0.94
MS2	40	$685.80 \pm 0.63_f$	0.22 ± 0.01	0.98
MS3	60	$796.40 \pm 0.94_c$	0.14 ± 0.009	0.99
MS4	80	$784.20 \pm 0.22_d$	0.18 ± 0.002	0.99
MS5	100	$874.30 \pm 0.08_a$	0.23 ± 0.006	0.99
MS6	120	$867.90 \pm 0.19_b$	0.16 ± 0.004	0.99

Table 4.11 displays the consistency index (K) and flow behaviour index (n) values that were calculated using the power law model. Shear thinning characteristics ($n < 1$) and non-Newtonian behaviour were seen in all mayonnaise samples, suggesting a pseudoplastic nature. The K values of all samples from MS1-MS6 (709.11 ± 0.04 to 867.90 ± 0.19) were significantly higher than that of the control (670.01 ± 0.75) mayonnaise sample ($p < 0.05$). The K value indicates the viscosity of the fluid, with higher values indicating a stronger emulsion structure. A decrease in viscosity can be attributed to an increase in shear rate, which overcomes Brownian motion and results in a decreased flow. A lower value of n signifies stronger shear thinning behaviour (Akcicek et al., 2022). The shear-thinning behaviour observed in mayonnaise may also result from the disintegration of connections between compounds (Erçelebi & Ibanouglu, 2009). Nanocellulose, a stabilizer in mayonnaise, forms hydrogen bonds with water and potentially with β-carotene, while its hydrophobic regions interact with both β-carotene and the hydrophobic components of oil droplets through hydrophobic interactions. As β-carotene is hydrophobic, it partitions into the oil phase and interacts with oil droplets via hydrophobic interactions, collectively contributing to the stability of the emulsion. Additionally, nanocellulose present in PNE provides outstanding resistance to droplet movement, which reduces the size of oil droplets

by avoiding coalescence (Ozdemir et al., 2021). Moreover, the increased β-carotene content in nanocellulose-stabilized mayonnaise led to a higher consistency index (K), which indicated the formation of a stronger network structure between droplets, contributing to the higher viscosity of the mayonnaise (Zhang et al., 2020).

4.3.4.6. RP-HPLC analysis of functional mayonnaise

The β-carotene present in the mayonnaise samples was analysed using HPLC. As shown in **Fig. 4.11**, the peak appearing between 30-35 min retention time correspond to the retention time of the β-carotene in each mayonnaise sample. In our experiment, which was performed under uniform determination procedures, the content of β-carotene increased with the increase in the concentration from MS1 to MS6. As the concentration increased, the peak areas increased. The peak area represents the quantity of compounds that has passed through the detector. **Table 4.12.** shows the amount of β-carotene concentration present in the mayonnaise samples. The highest concentration was found in MS6 sample of mayonnaise, where the peak height was highest, which proved that there was no degradation of β-carotene in the nanocellulose stabilized mayonnaise. Studies have proven that combining rutin and whey protein isolate stabilized β-carotene emulsions exhibited enhanced bioaccessibility and offered potential for functional food and nutraceutical applications (Li et al., 2023). Novel Pickering emulsions, co-stabilized by solid particles and lactoferrin or rhamnolipid emulsifiers, enhanced β-carotene entrapment, and stability, while slightly reducing its bioaccessibility during in vitro digestion (Wei et al., 2020). Therefore, in the present study, the BRNC stabilised PNE which was used to make mayonnaise does not have any adverse effect on the β-carotene added to the mayonnaise sample, which makes it an ideal stabilizer for developing bioactive rich health promoting mayonnaise.

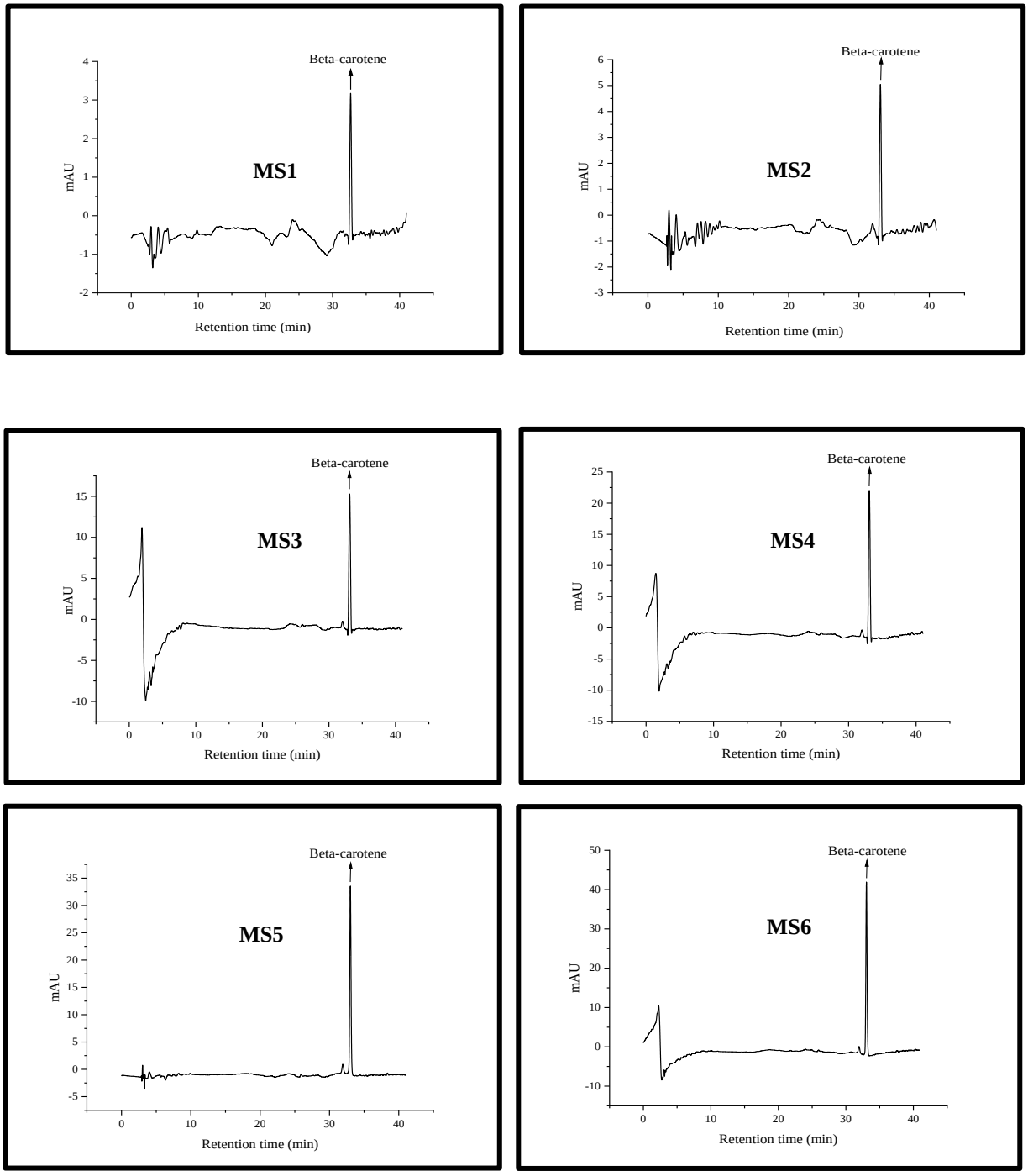

Fig. 4.11. HPLC chromatograms of β-carotene present in mayonnaise samples.

Table 4.12. Quantification of identified β-carotene in mayonnaise extract

Sl. No.	Samples	β-carotene (µg/100g)
1	MS1	7.68±0.13
2	MS2	16.68±0.04
3	MS3	38.16±0.22
4	MS4	43.15±0.17
5	MS5	54.32±0.02
6	MS6	61.26±0.08

4.3.4.7. In-vitro lipid digestion

The lipid digestion in mayonnaise samples (MS1 to MS6) decreased in both rate and extent as the concentration of cellulose nanoparticles increased (**Fig. 4.12**). This reduction is attributed to the formation of a dense interfacial film around the oil droplets, which results from the inclusion of Pickering nanoemulsions (PNE) in the mayonnaise. The cellulose nanoparticles in PNE act as stabilizers at the oil-water interface, forming a physical barrier that inhibits the action of lipase enzymes on the oil. Consequently, the enzymes are less able to access the lipid substrates, leading to a decrease in lipid breakdown. As the concentration of nanoparticles increases, the barrier becomes denser, further limiting enzyme access and slowing down the digestion process.

When mixed with simulated intestinal fluid (SIF), all mayonnaise samples followed a similar pattern of free fatty acids (FFAs) release: a rapid release during the first 30 minutes followed by a slower phase. However, the final release of FFAs varied based on the amount of PNE added. Cellulose nanoparticle-stabilized mayonnaise showed a slower release of fatty acids, primarily because it formed a gel structure during gastric digestion. This slower digestion is linked to changes in the emulsion structure after gastric digestion, where larger droplet aggregates were observed. Studies by Golding et al. (2011), Scheuble et al. (2018), and Du Le et al. (2020) support these findings, demonstrating that emulsion structure, particularly aggregation and droplet lump formation, significantly impacts the rate of intestinal lipolysis and fatty acid release.

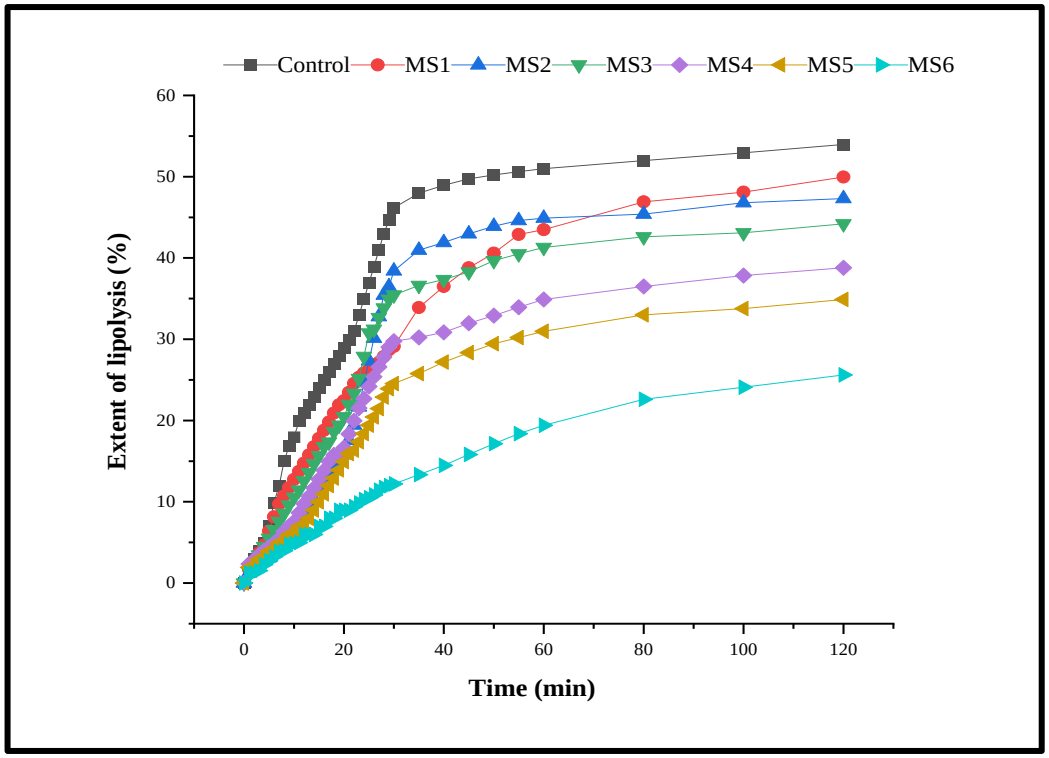

Fig. 4.12. Intestinal lipolysis profile of the mayonnaise samples stabilized by Pickering nanoemulsions.

The reduced digestion rate is explained by the fact that cellulose nanoparticles form a robust interfacial film around oil droplets, preventing lipase enzymes from accessing the oil. These nanoparticles adhere strongly to the oil-water interface and resist being displaced by bile salts due to their high desorption energy. Additionally, in the acidic and high-ionic-strength environment of the stomach, the nanoparticles form a gel structure, causing oil droplets to aggregate, further slowing the digestion process. Even after 2 h of digestion, some oil droplets remain encapsulated within the cellulose shell, indicating that the emulsion structure largely remains intact, thereby protecting the oil from complete digestion (Ni et al., 2021).

4.3.4.8. β-carotene bioaccessibility

Figure 4.13. shows the β-carotene bioaccessibility of mayonnaise samples after in-vitro digestion. The stability of a substance like β-carotene after digestion and its actual absorption by the body determine its health benefits. In order to guarantee that β-carotene may be efficiently absorbed and offer health advantages, it is imperative to investigate how encapsulation impacts its stability and absorbability during in vitro digestion. Because the

MS6 sample may shield β-carotene from deterioration in the acidic stomach environment, it has a higher β-carotene bioaccessibility, which indicates improved chemical stability. Additionally, MS6 had higher β-carotene bioaccessibility than MS1, possibly as a result of the MS6 sample structure's superior ability to retain β-carotene after digestion. Despite reduced lipolysis rates, this enhanced retention results in increased β-carotene bioavailability (Qi et al., 2020).

The bioaccessibility of β-carotene was found to be significantly higher in MS6 (48.1%) compared to MS1 (24.5%), which may be attributed to differences in the emulsion structure between the two samples. In MS6, the structure appears to better preserve the integrity of β-carotene during digestion, potentially due to the higher concentration of cellulose nanoparticles forming a more stable interfacial film around the oil droplets. This protective barrier likely prevents extensive oxidation or degradation of β-carotene in the harsh gastric and intestinal environments, allowing more β-carotene to be released and absorbed (Yi et al., 2021). In contrast, MS1, with a lower concentration of nanoparticles, offers less protection to the β-carotene, leading to lower bioaccessibility. This suggests that the emulsion stability and structure play a critical role in enhancing the bioavailability of β-carotene during digestion.

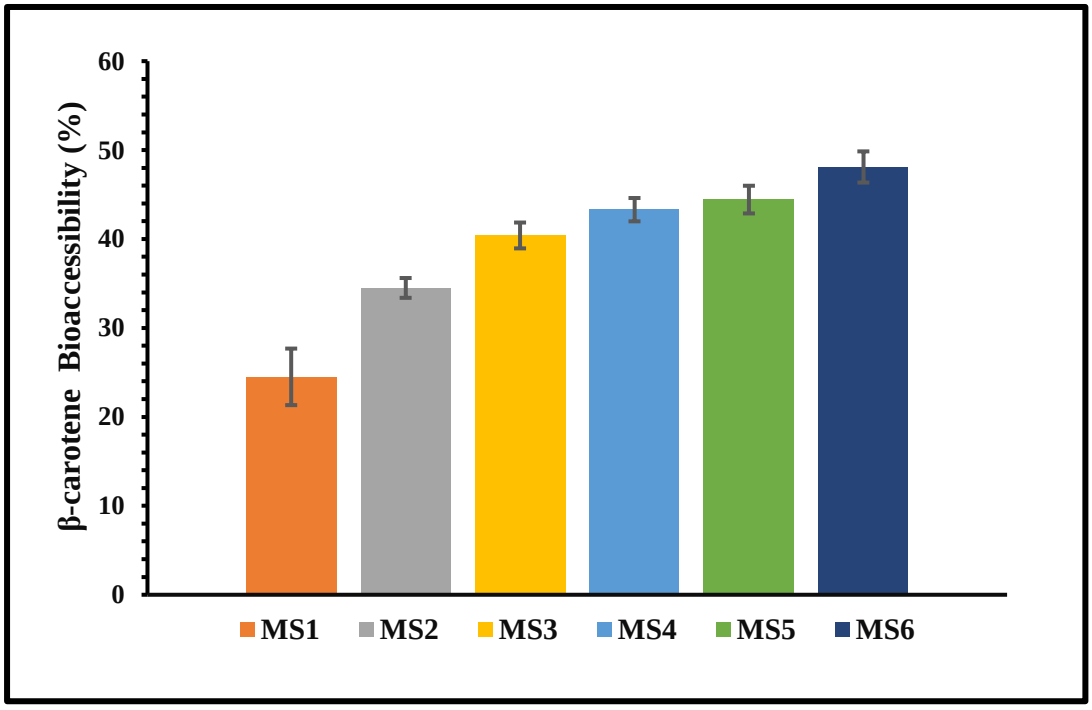

Fig. 4.13. β-carotene bioaccessibility of mayonnaise samples after in-vitro digestion.

4.4. Conclusion

The study conclusively demonstrates the efficacy of banana rachis nanocellulose (BRNC) as a natural, eco-friendly stabilizer for Pickering nanoemulsions (PNE) in food systems, specifically in enhancing the stability of hydrophobic bioactive compounds like β-carotene. BRNC's unique physicochemical properties, including its surface charge, hydrophilic-hydrophobic balance, biodegradability, and biocompatibility, significantly improved the stability of PNE, which had a particle size of 204 nm and a PDI of 1.722 and remained stable for 35 days. The encapsulated β-carotene in the PNE showed enhanced chemical stability with a retention rate of 0.81. Incorporating BRNC-based PNE into β-carotene-infused mayonnaise successfully improved its oxidative stability, rheological properties ($R^2 = 0.99$), textural attributes, and color stability. HPLC analysis confirmed the β-carotene content as 61.26±0.08 μg per 100 g of mayonnaise. Additionally, the PNE-stabilized mayonnaise demonstrated enhanced resistance to phase separation and prevented hydroperoxide formation throughout the analysis period. The inclusion of BRNC also contributed to reduced fat content while improving the functional properties of the mayonnaise. The study further showed that lipid digestion in mayonnaise decreased with increasing concentrations of PNE, as cellulose nanoparticles formed a dense interfacial film around oil droplets, blocking lipase enzymes. β-carotene bioaccessibility was notably higher in MS6 (48.1%) than in MS1 (24.5%), likely due to the improved structural protection provided by the PNE. Overall, this research highlights the potential of BRNC as a versatile and sustainable stabilizing agent in the food industry, contributing to the development of functional food products with enhanced stability, nutritional value, and eco-friendly properties. By valorizing agricultural waste into an effective stabilizer, this study offers a sustainable approach to food innovation, paving the way for healthier and more stable food formulations.